RESEARCH ON MACHINE VISION ROUNDNESS DETECTION METHOD BASED ON SNAKE ALGORITHM

Beiyi WANG[1]*, Yuting YAN[2]

In order to reduce the hardware cost of roundness detection, a machine vision-based roundness detection method is proposed. The basic idea of this roundness detection method is to divide roundness detection into two stages: coarse positioning and fine positioning. In the first stage, the Hough transform method is used to achieve rough localization of circular boundaries; In the second stage, the Snake algorithm is used to achieve precise positioning of circular boundaries. In the experimental verification stage, a circular instrument was used as the experimental object for experimental research, and a roundness detection effect evaluation method based on the least squares method was proposed. The experimental results show that the proposed method achieves ideal detection accuracy for circular features. Further selection of multi-attribute decision-making methods, decision tree methods, and support vector machine methods were compared with the proposed method for roundness detection, and the results showed that the proposed method can obtain higher accuracy roundness detection results.

Keywords: Roundness Detection, Machine Vision, Snake Algorithm, Least Squares Circle

1. Introduction

It is theoretically feasible for machine vision to complete the detection of small hole roundness features in mechanical parts [1-2]. Image processing techniques such as Hough transform and contour extraction can locate circular features of small holes at pixel or even sub pixel levels, and then extract the contours of circular hole features to evaluate their roundness. Obviously, if a machine vision based small hole roundness detection method can be constructed, it is of great significance for improving detection accuracy and efficiency [3-4].

The object of roundness detection is roundness error. The so-called roundness error refers to the difference between the true contour size shape and the ideal contour size shape of the shaft section of rotating parts. Roundness error is a very common and important type of error in rotating parts, which directly

[1] Associate Professor, New Quality Productivity and Career Development Institute, Guangdong Polytechnic, Foshan, 528041, China, e-mail: wangbeiyi@gdpt.edu.cn
[2] Research Assistant, New Quality Productivity and Career Development Institute, Guangdong Polytechnic, Foshan, 528041, China, e-mail: yanyuting@gdpt.edu.cn

affects the accuracy of the centering position, rotating motion, and hole axis fit of the parts. The inner surface of a circular small hole in a part must undergo roundness error detection under certain precision requirements [5-6].

Patino summarized the detection methods for roundness errors and divided them into two categories: contact roundness error detection methods and non-contact roundness error detection methods [7]. Cao pointed out that different classification standards can form different classifications, such as passive roundness error detection method and active roundness error detection method, offline roundness error detection method and online roundness error detection method, single technology operation mode roundness error detection method, and multi technology combination mode roundness error detection method [8-10]. In this article, the existing circular error detection methods are divided into two categories to elaborate, namely: hardware based circular error detection methods and software based circular error detection methods.

Roundness error measuring instrument is a type of canonical equipment for measuring roundness error [11]. Raj believes that in the fields of precision machining and manufacturing, roundness error measuring instruments are one of the important detection equipment [12]. The roundness error measuring instrument has many advantages: it is suitable for measuring various form and position errors, and the range of measurement objects is very wide [13]. High measurement accuracy, suitable for high-precision roundness detection [14]. It can be connected to digital control devices such as computers to achieve automation and intelligent data processing in the measurement process. Of course, roundness error measuring instruments also have some drawbacks: their prices are too high and are not suitable for small mechanical processing enterprises; There are high requirements for the testing environment and the operational skills of workers. Revilla pointed out that compared to specialized roundness error measuring instruments, coordinate measuring machines are a semi specialized roundness error measuring device [15]. When using a coordinate measuring machine to measure roundness error, it is necessary to measure a certain number of three-dimensional coordinates of points from the roundness features of the measured object, and then use spatial Cartesian coordinate method combined with some data processing method to calculate the roundness error of the measured object [16].

Pozner pointed out that laser measurement methods are a classic software-based roundness error detection method that requires the use of lasers as measuring devices during the measurement process [17]. The laser emits a laser to irradiate the tested object, and then the laser irradiation area is captured using image capture devices such as cameras. Then, image processing techniques are used to calculate variables that can characterize roundness error. In laser measurement methods, radius is the main variable that characterizes roundness error. In order to measure the changes in radius, laser measurement methods have

three different operating schemes: triangulation measurement, scanning measurement, and diffraction measurement [18]. Among them, the triangulation method utilizes the diffuse reflection principle of laser irradiation to calculate the change in radius and complete roundness error detection. Gan found that both scanning measurement and diffraction measurement methods use a strategy of constraining laser fringes, allowing the laser to be emitted from the slit to the measured object, thereby completing the calculation of radius changes to detect roundness errors [19]. Saif believes that machine vision measurement method is also a software centered roundness error detection method and a typical non-contact measurement method, but it does not require additional structural light sources such as lasers, only natural ambient light. Therefore, compared to laser measurement methods, machine vision measurement methods have significant cost advantages [20]. Machine vision measurement methods have many outstanding advantages: they do not need to be in contact with the measured object and are typical non-contact measurements; It can be used in natural light environments without the need for special structured light sources; The measurement system is simple and only requires a regular camera; Convenient to achieve automation and online measurement process, and convenient connection with digital processing equipment such as computers; With software programs as the core, the calculation process is easy to expand and improve, and has stronger adaptability for different roundness error measurement problems.

In this article, we take machine vision algorithms as the basic framework, combines Snake algorithm and Hough transform technology to construct a roundness detection method for machine vision, and verifies its effectiveness through experiments. Compared with previous research results, our method avoids the use of special hardware and achieves higher precision roundness detection through the combination of Snake algorithm and Hough transform technology.

2. Proposed Method

2.1 Method Flow

Taking the automatic recognition of disk instruments as an example, it relies on accurate positioning of circular features, scale features, and pointer features. Among them, accurate positioning of circular features is the foundation of the entire recognition work. The Hough transform is effective in detecting circular features, but the image is affected by factors such as noise and highlights, which can cause ghosting and other issues in Hough transform detection. Therefore, based on the Hough transform, this article further introduces and improves the Snake algorithm to accurately locate circular features.

Under this approach, the implementation process of the automatic recognition algorithm for disk instruments is presented, as shown in Fig. 1.

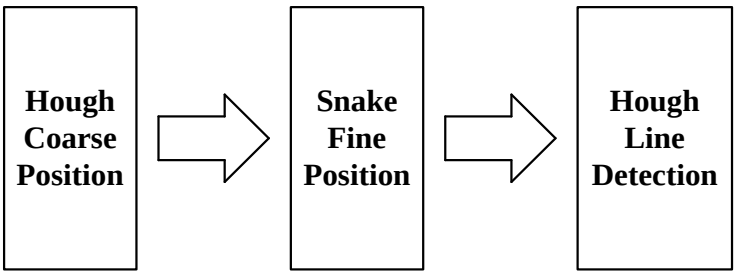

Fig. 1. Method flow of this article

In the algorithm flow shown in Fig. 1, the automatic recognition algorithm of the disk instrument is divided into three steps. The first step is to use Hough transform to roughly locate the circle, the second step is to use Snake algorithm to precisely locate the circle, and the third step is to use Hough transform to detect the scale and pointer. By combining the results of the above three steps, the indication of the disk instrument can be identified.

2.2 Hough Transform Coarse Positioning Circle

When edge detection and other methods are used to obtain curve features in instrument images, Hough transform can be used to locate circular features within them. The idea of Hough transform for detecting circular features is shown in Fig. 2. Assuming Hough transform processing of curve features, starting from point A.

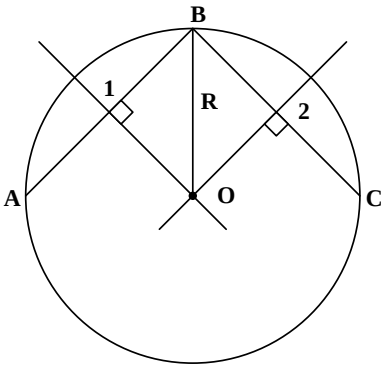

Fig. 2. Hough roundness detection principle

Along the arc direction of the curve, take point B at n intervals and point C at n intervals.

In this way, the midpoint coordinates of AB and BC segments can be calculated separately, as shown in formulas (1) and (2).

$$x_1 = \frac{x_A + x_B}{2}, y_1 = \frac{y_A + y_B}{2} \tag{1}$$

$$x_2 = \frac{x_B + x_C}{2}, y_2 = \frac{y_B + y_C}{2} \tag{2}$$

Through these two points, the normal equations of AB and BC segments can be written separately, as shown in formulas (3) and (4).

$$(x-x_1)(x_B-x_A)+(y-y_1)(y_B-y_A)=0 \tag{3}$$

$$(x-x_2)(x_C-x_B)+(y-y_2)(y_C-y_B)=0 \tag{4}$$

According to formulas (3) and (4), the intersection point of these two lines can be determined. According to the accumulation detection principle of Hough transform, for each intersection obtained, it is stored. If this intersection occurs repeatedly, accumulation is performed. Finally, the intersection point with the highest cumulative value will serve as the center of the circle, and the mean distance from the center to the points on each curve will serve as the radius, from which the circle detected by Hough transform can be obtained. The calculation of radius is shown in formula (5).

$$R=\frac{\sum_{i=1}^{n}\sqrt{(x_i-x_O)^2+(y_i-y_O)^2}}{n} \tag{5}$$

However, due to factors such as image noise and blurring, the circular features of ghosting will be detected by Hough transform, so this is a coarse localization method.

2.3 Snake Algorithm for Precise Positioning of Circles

The Snake algorithm gradually adjusts the position of the contour curve through the control of internal and external energy parameters, thus effectively solving the ghosting problem.

To use $Z(s)=(x(s),y(s))$ represent the curve adjusted by the Snake algorithm, define an overall energy adjustment function as follows:

$$F_{snake}=\int_0^1[F_N(Z(s))+F_W(Z(s))]ds \tag{6}$$

Here, $F_N(Z(s))$ represents the internal energy adjustment function and $F_W(Z(s))$ represents the external energy adjustment function, and their mathematical forms are as follows:

$$F_N(Z(s))=\frac{1}{2}\left[\varepsilon(s)\left|\frac{\partial Z}{\partial s}\right|^2+\sigma(s)\left|\frac{\partial^2 Z}{\partial s}\right|^2\right] \tag{7}$$

Here, $\varepsilon(s)$ represents the elastic parameter and $\sigma(s)$ represents the rigid parameter. The adjustment of internal energy depends on the curve itself. The larger the curvature of the curve, the greater its internal energy, and vice versa.

$$F_W(x,y))=-\left|\nabla J(x,y)\right|^2 \tag{8}$$

Here, ∇ represents gradient calculation and $J(x,y)$ represents the image.

Most of the captured images contain noise. Considering the use of Gaussian smoothing technology, the external energy adjustment function can be rewritten as follows:

$$F_W(x,y)) = -\left|\nabla[G_\sigma(x,y) * J(x,y)]\right|^2 \tag{9}$$

Here, $G_\sigma(x,y)$ represents the Gaussian smoothing function. The external energy adjustment function depends on the large number of boundary features present in the image.

At this point, a functional model corresponding to the Snake algorithm can be constructed, and the process of the Snake algorithm is the process of obtaining the minimum solution of this model. The Snake functional model is shown in formula (10).

$$\frac{\partial}{\partial s}\left(\varepsilon\frac{\partial Z}{\partial s}\right) - \frac{\partial^2}{\partial s^2}\left(\sigma\frac{\partial^2 Z}{\partial s^2}\right) - \nabla F_W = 0 \tag{10}$$

Further set the internal force and external force parameters to express the corresponding part of formula (10). The internal force parameters are shown in formula (11), and the external force parameters are shown in formula (12).

$$G_N = \frac{\partial}{\partial s}\left(\varepsilon\frac{\partial Z}{\partial s}\right) - \frac{\partial^2}{\partial s^2}\left(\sigma\frac{\partial^2 Z}{\partial s^2}\right) \tag{11}$$

The function of internal force parameters is to smoothly adjust the Snake curve.

$$G_W = -\nabla F_W \tag{12}$$

The action of external force parameters causes the Snake curve to collapse and approach towards the target contour.

When performing iterative processing, the Snake algorithm needs to further introduce time variables, resulting in the following form:

$$\frac{\partial Z}{\partial t} = \frac{\partial}{\partial s}\left(\varepsilon\frac{\partial Z}{\partial s}\right) - \frac{\partial^2}{\partial s^2}\left(\sigma\frac{\partial^2 Z}{\partial s}\right) - \nabla F_W \tag{13}$$

According to formula (13), the optimization goal of the Snake algorithm is to adjust the curve so that $\frac{\partial Z}{\partial t} \to 0$.

In the disk instrument recognition method constructed in this article, due to the limitations of Hough transform coarse positioning, the Snake algorithm has a smaller search area and can detect the precise position of the circle faster.

3. Experimental Results and Analysis

3.1 Basic Experiments

In order to verify the effectiveness of the roundness detection method

based on the improved Snake algorithm proposed in this chapter, experimental research was conducted on blurred part images. The experimental results are shown in Fig. 3.

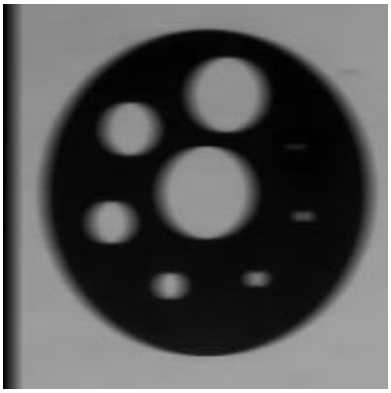

(a) Gaussian filter result

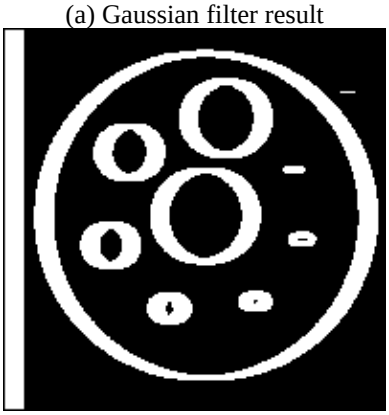

(b) Boundary regions detected by Hough transform

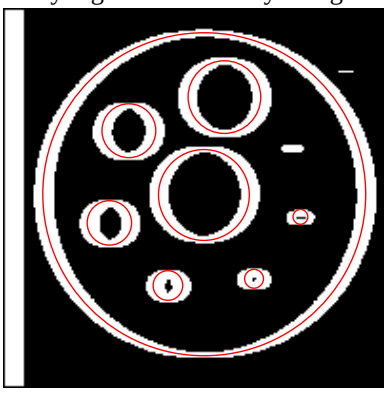

(c) Improved Snake algorithm for detecting boundaries

Fig. 3. Basic experimental results

Fig. 3 (a) shows the effect of noise removal using Gaussian filter; Fig. 3 (b) shows the boundary region detected by Hough transform; Fig. 3 (c) shows the

boundaries detected by the improved Snake algorithm. From Fig. 3 (a), it can be seen that due to issues such as relative motion between the parts and the camera during the shooting process, the mechanical parts have a blurring effect, which affects the accurate positioning of the circular boundary of the small hole. After the effect of Gaussian filter, the Gaussian noise in the original blurred image can be removed. From Fig. 3 (b), it can be seen that the Hough transform detects double boundaries for circular features in blurred images, and the areas between the double boundaries are marked as the detection areas of the Snake algorithm. From Fig. 3 (c), it can be seen that the limit boundary detected by the Hough transform is set as the initial contour curve of the Snake algorithm iteration process, and then the improved Snake algorithm is executed to locate the precise circular boundary of all small hole features.

3.2 Evaluation of Roundness Detection Effect in Basic Experiments

The circular boundary of the small hole feature, i.e. the position of the circularity feature, was detected in the basic experiment. So, how much error is caused by the roundness of small holes depends on the roundness evaluation method. To further evaluate the roundness of small hole features, it is necessary to perform least squares circle fitting based on this positional information. A schematic diagram of a least squares circle is shown in Fig. 4.

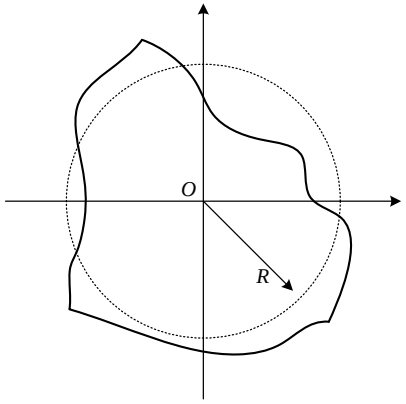

Fig. 4. Definition of least squares circle

As shown in Fig. 4, the thick solid lines represent the actual contour shape, while the dashed circles represent the least squares circles fitted based on the pixel positions of the actual contour. The center of the circle corresponding to this least squares circle satisfies the constraint of least squares, that is, the sum of squares of the distances from each pixel on the curve contour to the center of the circle is the minimum.

Assuming that the coordinates of any pixel on the curve contour can be described as (x, y), the center coordinates of the fitted least squares circle can be described as (K_x, K_y), and the radius of the fitted least squares circle can be expressed as R_k, then the fitted least squares circle satisfies the following equation, as shown in formula (4-2).

$$(x-K_x)^2+(y-K_y)^2=R_k^2 \tag{14}$$

Further rewrite the least squares circular equation shown in formula (14) into the ordinary polynomial form, as shown in formula (15).

$$x^2+y^2+mx+ny+p=0 \tag{15}$$

The three parameters in formula (15) satisfy the following relationship:

$$\begin{cases} m=-2K_x \\ n=-2K_y \\ p=K_x^2+K_y^2-R_k^2 \end{cases} \tag{16}$$

Of course, all pixels on the curve contour cannot all comply with formula (16). Assuming that the coordinates of the second pixel can be used (x_i, y_i) to represent it, a further deviation can be set as:

$$q_i=x_i^2+y_i^2+mx_i+ny_i+p=0 \tag{17}$$

In the above deviation expression, different deviations may have symbol differences, but because all pixels of the contour correspond to the random error characteristics of the least squares circle, the possible impact of symbols is not considered here.

According to the iterative principle of least squares, the sum of squared deviations of all pixels on the curve contour should be minimized. To achieve this, set the following iterative function:

$$F(m,n,p)=\sum_{i=1}^{n}q_i^2=\sum_{i=1}^{n}(x_i^2+y_i^2+mx_i+ny_i+p)^2 \tag{18}$$

The objectives of the least squares optimization iteration are as follows:

$$\min\{F(m,n,p)\} \tag{19}$$

In order to achieve the minimum value of a ternary function $F(m,n,p)$, the following conditions should be met:

$$\begin{cases} \dfrac{\partial F(m,n,p)}{\partial m} = 0 \\ \dfrac{\partial F(m,n,p)}{\partial n} = 0 \\ \dfrac{\partial F(m,n,p)}{\partial p} = 0 \end{cases} \tag{20}$$

Of course, the circle calculated by this solution does not guarantee that all pixels of the curve contour are traversed by this circle. However, this circle ensures that the sum of squares of the distances between all pixels on the curve contour and the center of the circle is minimized.

Further provide the calculation results of the center and radius of the least squares circle, as shown in formula (21).

$$\begin{cases} K_x = -\dfrac{m}{2} \\ K_y = -\dfrac{n}{2} \\ R_k = \sqrt{K_x^2 + K_y^2 - p} \end{cases} \tag{21}$$

Once the least squares circle is determined, the distance between each pixel on the curve contour and the center of the circle can be calculated, and then the mean of this data for all pixel points can be calculated. The roundness error result of this small hole can be calculated, completing the roundness evaluation work.

By using the improved Hough transform roundness detection method, all small hole features in mechanical part images were obtained. Further label it in the following form, as shown in Fig. 5.

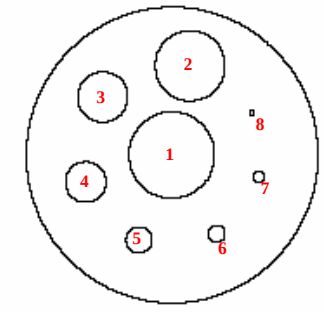

Fig. 5. Annotation of normal image roundness detection results

From Fig. 5, it can be seen that the largest small hole in the center is labeled as the 1st space, and then the 7 external small holes are labeled counterclockwise, resulting in a total of 8 small hole features being labeled.

Using the least squares roundness evaluation method, perform roundness evaluation on the 8 small holes in Fig. 5, and the evaluation results are shown in the curve in Fig. 6 and the data in Table 1.

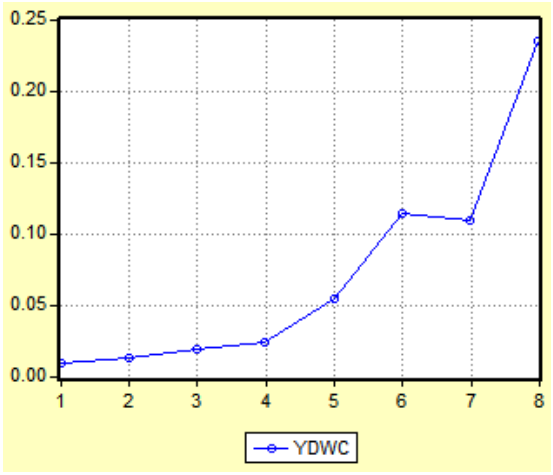

Fig. 6. Roundness evaluation curve of small holes in normal images

Table 1

Evaluation Results of Roundness of Small Holes in Normal Images

Small hole label	Roundness error
Hole 1	0.0089
Hole 2	0.0133
Hole 3	0.0194
Hole 4	0.0235
Hole 5	0.0548
Hole 6	0.1142
Hole 7	0.1087
Hole 8	0.2352

Based on the data results in Table 1 and the curve results in Fig. 6, it can be seen that for normal mechanical part images, the improved Hough transform roundness detection method can accurately locate the small hole circular feature boundary; When the size of the small hole is large enough, its roundness error is relatively low; As the size of the small hole decreases, the image resolution in the small hole area is insufficient, resulting in less pixel information and an increase

in roundness error. The above results also fully demonstrate that the least squares roundness evaluation method can provide a more accurate evaluation of small hole roundness.

3.3 Practical Roundness Detection Application Experiment

In order to further verify the application effect of this method in actual roundness detection, the following experimental research is conducted. Take an image of a mechanical pressure gauge as the experimental image (as shown in Fig. 7 (a)), first perform grayscale processing (as shown in Fig. 7 (b)), then filter and denoise it (as shown in Fig. 7 (c)), then perform Hough transform coarse positioning (as shown in Fig. 7 (d)), and finally achieve Snake fine positioning (as shown in Fig. 7 (e)).

(a) Original image (b) grayscale image (c) denoised image

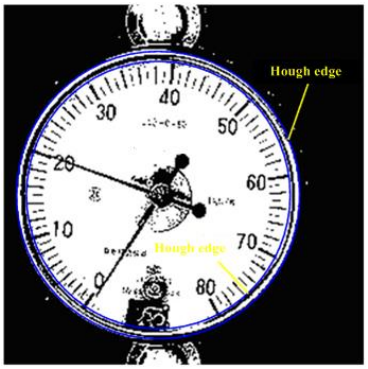

(d)Hough coarse positioning

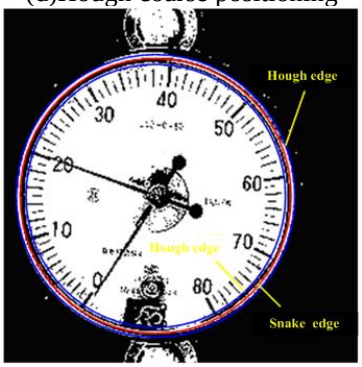

(e)Snake fine positioning

Fig. 7. Experimental results of practical application

From the results in Fig. 7, it can be seen that due to factors such as halo, multiple circular and arc features appear in the instrument disk area. The Hough transform detected the region where this circular feature appeared, thereby determining the outer and inner boundaries, reducing the scope for the Snake algorithm's precise localization. The Snake algorithm locates features such as circle boundaries and centers, providing assistance for Hough transform in detecting line features, thereby determining line features such as pointers and scales. The experimental results fully demonstrate that the method proposed in this article effectively achieves the detection target in the detection of disk instruments.

In order to make a horizontal comparison with the method proposed in this paper, the roundness detection errors generated by the four methods are compared with the multi-attribute detection method (MAD), decision tree detection method (DT) and support vector machine detection method (SVM). We used a standard image dataset consisting of circular objects of different shapes, sizes, and positions, all done on the same computer, based on multiple sets of experiments. By comparing the accuracy of different algorithms in roundness detection, we find that the Snake algorithm combined with the Hough transform has a significant improvement in accuracy, and its speed and stability are not reduced. The results are shown in Table 2.

Table 2

Roundness Error Detection Results of Four Methods

Method	Roundness detection error
MAD	5.68%
DT	4.69%
SVM	4.31%
Ours	2.36%

We conducted repeated tests on each set of experimental data to ensure the reliability of the experimental results. By calculating the mean value and standard deviation, we verify the stability and consistency of the experimental results. The results show that the difference between the data of each group is within the acceptable range, which proves the reliability of the experimental results. As can be seen from the comparison results in Table 2, the proposed method has the smallest error in roundness detection and is superior to the other three methods. This method has excellent performance in accuracy, speed and stability, providing a new and effective way to solve the roundness detection problem.

4. Conclusions

The combination of Hough transform and Snake algorithm shows remarkable synergistic effect in roundness detection. The Hough transform provides an effective preliminary location for the circular target, while the Snake algorithm further realizes the accurate outline of the boundary. This fusion strategy not only significantly improves the accuracy of detection, but also enhances the stability of the algorithm in the variable and complex environment. Through comparative experimental evaluation, we found that this combined method has improved accuracy, operation speed and system stability compared with a single Hough transform or Snake algorithm. Especially when dealing with images containing complex background and noise interference, the method can still maintain high detection accuracy, which fully proves its wide potential and practical value in practical applications. In addition, the roundness detection method proposed in this study shows wide applicability. This method can provide accurate and reliable detection results for precise detection on industrial production lines or lesion location in medical image analysis and provides strong technical support for different application scenarios in different fields.

Looking forward to the future, we believe that by introducing advanced image preprocessing technology, we can further reduce the noise interference and improve the processing ability of the algorithm for complex background. At the same time, combined with modern technologies such as deep learning, Snake algorithm is expected to be improved to further improve its accuracy and robustness. In order to meet the needs of real-time detection, we will explore techniques such as parallel computing and hardware acceleration to improve the execution speed of algorithms. Using GPU for parallel computation will be a worthwhile direction to try, which can significantly speed up image processing and enable algorithms to complete detection tasks faster. In addition to roundness detection, the method proposed in this study has the potential to be extended to other shape detection fields. By adjusting the parameters and shape model of Snake algorithm, we can apply it to the detection of ellipses, rectangles and other shapes to provide solutions for more practical problems. In addition, we look forward to integrating the roundness detection method proposed in this study into existing machine vision systems to achieve more efficient and accurate automated detection. By combining with other image processing algorithms and sensor technologies, a more intelligent and flexible machine vision system is built to provide more comprehensive technical support for industrial production, medical diagnosis and other fields.

Acknowledgments

This paper is supported Foshan Key Laboratory of Textile and Garment Design and Intelligent Manufacturing Technology under grant No. FS2024011.

R E F E R E N C E S

[1]. Vasanth S, Muthuramalingam T, Gupta S. Carbonization Region Measurement in Vegetable Tanned Goat Leather using Machine Vision System for Evaluating Performance Measures of Leather Cut Contour Edges. Journal of the American Leather Chemists Association, 2022, 17(2): 1171-1178.

[2]. Xing-Fang A, Ren-Huang W, Xue-Chen L. The Application of Roundness Error Measurement in the Detection of Badminton Appearance. Journal of Guangdong University of Technology, 2011, 25(6): 1-10.

[3]. Ye H. Intelligent Image Processing Technology for Badminton Robot under Machine Vision of Internet of Things. International Journal of Humanoid Robotics, 2022, 32(6): 558-571.

[4]. Gong Y, Huang Z. Research on Sub Pixel Roundness Detection Technology Based on B-spline Lifting Wavelet. Atlantis Press, 2015, 24(8): 1-11.

[5]. Li P, Zhou L, Feng X, et al. Application of Roundness Test on Tires Based on Five – Point Cubic Smoothing Algorithm. IOP Conference Series Materials Science and Engineering, 2018, 38(1): 122-131.

[6]. Kong G, Zong Z, Yang J, et al. Roundness error separation based on singularity detection and exact-stop of spindle in on-machine measurement of spindle rotation error. Mechanical Systems and Signal Processing, 2022, 169:108-116.

[7]. Patino-Alonso C, M Gómez-Sánchez, L Gómez-Sánchez, et al. Predictive Ability of Machine-Learning Methods for Vitamin D Deficiency Prediction by Anthropometric Parameters. Mathematics, 2022, 10(3): 608-617.

[8]. Cao W, Wang D, Cui G, et al. Analysis of the roundness error elimination in counter-rotating electrochemical machining. Journal of manufacturing processes, 2022, 76(4): 1028-1037.

[9]. Cai H Y, Wang Z, Wang W T, et al. Design of Tire Roundness Error Detection System. Opto-Electronic Engineering, 2010, 37(10):41-46.

[10]. Shanqi C, Hua Z, Yang L, et al. Study on laser online detection technology of roundness for small diameter shaft and pipe parts. China Metal Forming Equipment & Manufacturing Technology, 2015, 23(2): 111-120.

[11]. Bin Z. On application of least square method in space roundness detection. Shanxi Architecture, 2013, 33(6): 68-75.

[12]. Raj, Arun P. Ravi, Avneesh Kumar Dhanish, P. B. Factors influencing the performance of a roundness measuring instrument - Development of an empirical model. Measurement, 2019, 33(10): 131-140.

[13]. Das N, Khan T, Das A, et al. A Novel Quinoline Derivative for Selective and Sensitive Visual Detection of PPB Level Cu 2+ in an Aqueous Solution. Current Analytical Chemistry, 2022(2):1-18.

[14]. Desai M P, Patil R V, Harke S S, et al. Bacterium Mediated Facile and Green Method for Optimized Biosynthesis of Gold Nanoparticles for Simple and Visual Detection of Two Metal Ions. Springer US, 2021(2): 1-9.

[15]. Barik B, Mohapatra S. Selective visual detection of histamine and ascorbic acid through the rapid gel-sol transition of luminescent alginate hydrogel. Sensors and Actuators, B. Chemical, 2022, 36(7): 1-10.

[16]. Salehipour P, Mahdiannasser M, Shayegan G S, et al. CRISPR-Based Fluorescent Reporter (CBFR) Assay for Sensitive, Specific, Inexpensive, and Visual Detection of a Specific EGFR Exon 19 Deletion in NSCLC. Molecular biotechnology, 2023, 35(1): 44-52.
[17]. Pozner J N, Cohen J L, Burns J, et al. State of laser resurfacing 2021: A roundtable discussion. Dermatological Reviews, 2021, 31(9): 18-28.
[18]. M Revilla-León, Rubenstein J, Methani M M, et al. Trueness and precision of complete-arch photogrammetry implant scanning assessed with a coordinate-measuring machine. Journal of Prosthetic Dentistry, 2021, 28(10): 453-462.
[19]. Gan Y, Duan C, Liu G, et al. Dynamic frequency scanning interferometry measurement based on optical frequency synchronous motion measurement and error compensation. Optics Communications, 2021, 48(8): 126-135.
[20]. Saif Y, Yusof Y, Latif K, et al. Roundness Holes' Measurement for milled workpiece using machine vision inspection system based on IoT structure: A case study. Measurement, 2022, 19(5): 1925-1931.